Geopersia 2026, 16(1): 1-18
DOI: 10.22059/geope.2025.385170.648787

RESEARCH PAPER

The impact of climate change and water resources management on the groundwater volume and chemistry of the Neyriz Aquifer

Somayeh Zarei Doudeji ,*

Faculty of Earth Sciences, Shahrood University of Technology, Iran

Received: 10 November 2024, Revised: 03 May 2025, Accepted: 26 May 2025

Abstract
Global warming and climate change have repeatedly led to droughts in arid and semi-arid regions such as Iran. When these droughts are compounded by poor management of groundwater resources, severe water crises occur. This leads to a deterioration of groundwater resources in terms of both quantity and quality. The excessive abstraction of groundwater for human consumption, e.g. for drinking, industrial and agricultural purposes, leads to a sharp decline in groundwater levels and ultimately to land subsidence. This study deals with the effects of climate change and the mismanagement of groundwater resources in the Neyriz plain. For the hydrogeological study, iso-potential and flowline maps from September 1995 to 2020, iso-EC lines from September 1998 to 2020, and hydrographs and chemograms of the aquifer were plotted along with Piper, Durov, Shoeller and Gibbs diagrams. The results indicate an annual drawdown of 0.4 meters in the plain and a decline in water quality from 1998 to 2020. The cross section along the aquifer in 1998 and 2020 reveals a reverse slope of the water level near the lake, which has led to surface saltwater intrusion into the aquifer from the lake that increasing by about 175 percent from 1998 to 2020. Since there are no geophysical surveys in the area, the depth of the bedrock was estimated based on the maximum depth of the nearby production wells. The volume of the aquifer was calculated using ArcGIS software for each year from 1995 to 2020 and an empirical equation was derived to predict the volume of the aquifer based on the water level of the plain in the present or in the future. Based on the relationship between groundwater level, EC and volume of the aquifer, it was found that the aquifer behaves differently when the level is above or below 1538 meters. It was found that below 1538 meters, the lateral surface of the aquifer in the western part decreases sharply, reducing the volume of the aquifer and increasing the infiltration of salt water from the lake. It is therefore recommended to carry out artificial recharge in the Neyriz Plain to prevent the water table from dropping especially bellow 1538 meters. In addition, the construction of an underground dam at the western part of the aquifer can effectively prevent saltwater intrusion from the lake. In addition, the thickness of the aquifer in the plain was plotted for selected years to observe changes over time. The results indicate that the aquifer boundary should be reassessed.

Keywords: : Aquifer thickness, Aquifer volume, Neyriz Plain, ArcGIS, Hydrogeology, Hydrochemistry

Introduction

In arid and semi-arid regions like Iran, the dependency on groundwater resources for human lives is very high (Li et al., 2013; Jolly et al., 2008). Among human needs (drinking, industry, agriculture, and animal husbandry), the need for drinking water is one of the most essential and strategic. Therefore, it is necessary to determine the volume of potable groundwater in each region to manage the water resources based on the preservation of these reserves for future generations.

* Corresponding author e-mail: s.zarei@shahroodut.ac.ir

The impact of climate change on groundwater resources has been studied in various researches (Franssen, 2009; Earman and Dettinger, 2011; Kumar, 2012; Gorelick et al., 2014; Guermazi et al., 2019; Hasan et al., 2022; Engelenburg et al., 2018). Lo´aiciga (2009) investigated the long-term climatic changes and sustainable groundwater resources management. He reviewed the long-term patterns of climate change, secular climatic variability, predicted population growth, their relation to water resources management, and means available for mitigating and adapting to trends of climatic change and variability and their impacts on groundwater resources. Ertürk et al. (2014) evaluated the impact of climate change on groundwater resources in a part of the Köyceğiz–Dalyan Watershed. They quantified the impacts of climate change on the water budget components and modeled it with SWAT. The results indicated that water scarcity is expected to be a problem in the future and recommended switching to more efficient irrigation methods and crops with lower water consumption. Shamir et al. (2014) investigated climate change and water resources management in the Upper Santa Cruz River, Arizona. They assessed the impact of projected climate change on regional water resources management and concluded that climate change projections increase uncertainty and further complicate water resources management. Ostad-Ali-Askari et al. (2019) used MODFLOW to investigate the effect of management strategies on reducing negative impacts of climate change on water resources. They predicted climate conditions for the future period of 2020 to 2024 under three groundwater sustainability management scenarios that included 10%, 30%, and 50% reduction in groundwater extraction. Their results showed that water abstraction from the aquifer should be reduced by up to 50% of the existing wells for sustainable aquifer management. Additionally, changing the irrigation method from surface to subdroplet irrigation caused a 40% reduction in water use for agriculture. Ahmadi et al. (2020) forecasted groundwater levels under climate change and water resources management scenarios in the Najafabad Plain in central Iran. They defined three management scenarios under two climate change scenarios, A2 and B1, and used trained ANN-PSO to project the effects of each scenario on the groundwater level in the plain. Felisa et al. (2022) researched the combined management of groundwater resources and water supply systems at a basin scale under climate change. They proposed a coupled approach combining groundwater models (MODFLOW) to investigate different stress scenarios involving climate change and anthropic activities, and water management models to assess water resources availability and the best long-term management strategy for large-scale water supply systems. They observed that coupling the two model types allows for evaluating water resources availability in connection with management rules, examining more realistic operation choices, and planning infrastructures at a basin scale. Ciampittiello et al. (2024) researched water resources management under climate change. They suggested and proposed solutions by scientists from around the world, tips, and ideas to deal with climate change, and presented the best solutions for future water management. Ashofteh et al. (2024) researched water resources management considering groundwater instability affected by climate change in the Khorramabad aquifer of Iran with an integrated model in WEAP software and compared their results with GMS software results. The allocation of surface water and groundwater resources to consumption sectors (agricultural, urban, and industrial sectors) was analyzed using WEAP. Results showed that the lowest deficit of water resources in all sectors occurred in RCP26 (2040–2069) with a value of 7% and the highest deficit occurred in RCP85 (2070–2099) with a value of 180% compared to the baseline. The groundwater storage and distribution in Uzbekistan aquifers were determined by ArcGIS techniques and borehole data utilization by Wahyuni et al. (2008), showing a groundwater storage of about 15.5 BCM (billion cubic meters). Al-Sheikh and Al-Shamma'a (2019) calculated the volume of water for the Al Dammam unconfined Aquifer using digital elevation models, thickness maps, and flow maps in the study area. Şimşek et al. (2020) estimated the total recharge and discharge of groundwater

using the ArcGIS-integrated water level fluctuation method in the Alaşehir aquifer in Turkey.

In the study area and its surroundings, Moradi and Nikzad (2022) examined human interaction with arid and semi-arid environments, comparing traditional methods of water management and exploitation in Neyriz Plain. Their results show a direct relationship between livelihood and water resource management patterns, significantly influencing the distribution and type of settlements (nomadic or sedentary). Saemi and Kamali (2009) investigated balance calculation methods and management of Neyriz Plain water resources, calculating groundwater balance in four geological structure zones in the plain. Results showed that only in zone 2 was the groundwater balance positive, while in all others, it was negative. Hosseini et al. (2020) examined the groundwater quality condition of HasanAbad-Dehchah plain northeast of Neyriz, revealing that brackish groundwater had penetrated fresh water between 2.7% and 50%. In this case, reverse cation exchange occurred, with brackish water being absorbed by aquifer particles and replaced by calcium and magnesium. Sorkhabi et al. (2022) found land subsidence and groundwater storage using multi-sensor and extended Kalman filter in Eij plain southwest of Fars province. They used interferometric synthetic aperture radar from 2014 to 2020, gravity recovery and climate experiment (GRACE) and GRACE-Follow on (GRACE-FO) from 2002 to 2020, and piezometric well (PW) data from 1993 to 2015 to study subsidence and groundwater storage (GWS). Their results showed that the maximum Eij subsidence was 16 cm/year, with subsidence around the sinkhole evaluated at about 8 cm/year. The water level had a decreasing linear trend of 1.91 m/year. Hedayat et al. (2021) studied the condition of groundwater resources in the plains of the Bakhtegan-Maharloo basin by analyzing the hydrographs of 19 plains in the basin. The aquifer hydrographs indicated that Arsanjan, Kavar-Maharloo, Seidan-Faroogh, Saadat Abad, and Ghare Bagh plains had the highest annual fall in groundwater levels, with drops of 2, 1.68, 1.19, 1.04, and 1.02 meters, respectively. Ghalamkar et al. (2019) evaluated groundwater resources by identifying the layered structure of the earth using the electrical field method in Runiz Plain, west of Estehban. They conducted 97 depth measurements using the Scherlomberger array to identify karst areas containing water in Roniz Plain.

This study investigates the hydrogeological and hydrochemical situation of Neyriz Plain in Iran, calculating the aquifer volume and its change during the statistical period of data. Equations for predicting aquifer volume and electric conductivity (EC) from aquifer water level in the future are also determined. The aquifer thickness of Neyriz Plain is calculated and plotted in selected years. Hydrochemical graphs like Piper, Schoeller, Durov, and Gibbs are plotted for hydrochemical interpretations. ArcGIS software is used to calculate the aquifer volume and thickness, as well as all plots in this research.

The study area is located in one of the sub-basins of Bakhtegan Lake in the south of Iran, between latitudes 29˚ 00′ to 29˚ 29′ and longitudes 53˚ 59′ to 54˚ 29′ in Fars province (Fig. 1). The maximum and minimum heights in the study area are 2818 and 1555 meters, respectively. Bakhtegan Lake is in the northwest of the study area (Fig. 1). The study area covers an area of about 995 km^2 and is situated on the margin of the large and main Zagros thrust. From a tectonic perspective, it is a fragmented area with extensive landslides. The study area is located in the Sanandaj-Sirjan zone of Iran, where igneous, metamorphic, and sedimentary facies can be observed side by side. The oldest and youngest outcropping formations in this area are the Hormoz formation and the Quaternary sediments. The eastern and northern elevations of the region are mainly covered by Cretaceous limestones without layering. These limestones, somewhat crystallized in some places, contain the fossil of Orbitulin, an indicator of the Lower Cretaceous. Cretaceous limestones can be seen in the eastern part of Zagros, and in the western part, outcrops of Gabbro, Peridotite, and Serpentine rocks can be seen, forming the colored mixtures of the region (color mélange). In the southern parts, there are Cretaceous limestones (Tarbur) and Jahrom limestones. The thickness of the sediments in the region varies significantly, with the alluvial sediments reaching a useful thickness of more than 100 meters (Aghanabati, 2004).

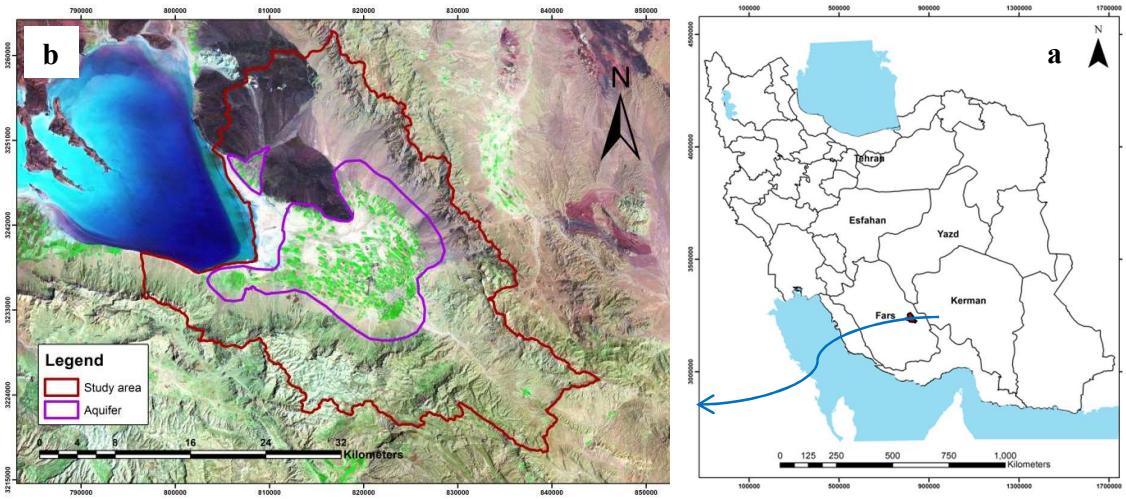

Figure 1. The location of study area in Iran (a) and in Landsat-7 satellite image (b)

The geological formations in the study area, in order of age, include the Hormuz salt dome formation, deposits from the second and third geological periods, and sediments from the present age. The Hormoz formation is in the southwest of the study area and has a negative effect on groundwater quality. Among the formations of the second geological period, the study area contains color mélange deposits with igneous materials and the limestones of the Tarbor Formation in Besh Mountain (Aghanabati, 2004). The mentioned limestone formation is one of the main sources of drinking water in Neyriz city (Fig. 2a).

Geophysical studies of this area were conducted in the form of Neyriz plain studies from 1964 to 1972. According to the results, the thickness of the alluvium varies from 30 meters at the edge of the heights to more than 120 meters in the west of Neyriz city. The bedrock of the plain consists of mixed colored deposits, igneous masses, and crystalline limestone from Triassic metamorphism, while in the northern areas of Neyriz city, it is made of red lotamite clays (Regional Water Company of Fars, 2020). For more precision in locating the bedrock (to better calculate aquifer volume and thickness), the maximum depth of the nearest alluvial wells (123 wells) was selected from 385 EWs located in the aquifer as the minimum probable bedrock depth (or maximum probable bedrock level), as illustrated in Fig. 2b. Meteorological data from this plain shows an annual average of rainfall, temperature, and evaporation at 245 mm, about 19 degrees, and 2531 mm, respectively (Regional Water Company of Fars, 2020). In this research, the aquifer boundary was obtained from the Regional Water Company of Fars.

Methodology

The article proposes methods for understanding the hydrogeological and hydrochemical situation of the Neyriz aquifer, including changes in aquifer thickness and volume and hydrochemistry over time. To calculate the aquifer thickness and volume, the maximum probable bedrock level is determined by the depth of the maximum exploitation wells (EWs) in the study area. Additionally, simple equation is proposed for calculating aquifer volume based on hydrograph water levels.

Hydrogeology and hydrochemistry approach

The Neyriz plain has an unconfined aquifer with a 234.9 square kilometer area, containing 22 observation wells (OWs) whose locations are shown in Fig.1b, and their parameters are detailed in Table 1. Water depths in these 22 OWs have been recorded from August 1995 to September

2020, with summarized data in Table 1 (Regional water company of Fars, 2020). Based on this data, OW P19 dried up in September 2009. This is further confirmed by the September 2020 data in Table 1. Table 1 also displays the average, maximum, and minimum water levels of each OW. Additionally, the EC values in 33 EWs have been recorded from September 1998 to September 2020 in the Neyriz plain, as outlined briefly in Table 2. Notably, the minimum EC value is 308 µS/cm in W9, while the maximum is 37310 µS/cm in W3. If one compares the maximum and minimum values of the EC in the aquifer with the results from Figure 3 and 4, it can be seen that EW of W9 is located at the front of the freshwater entry into the aquifer from the mountain side and W3 at the front of the salt water intrusion of the lake into the aquifer. Considering the high values of EC in the lake (Vahidipour et al., 2021), the existence of this difference between the maximum and minimum EC values of the aquifer seems natural. Table 3 presents the results of chemical analysis for groundwater samples from W1 to W15 of Table 2, taken in November 2004 and December 2018. These data are utilized to analyze the hydrogeological conditions of the study area.

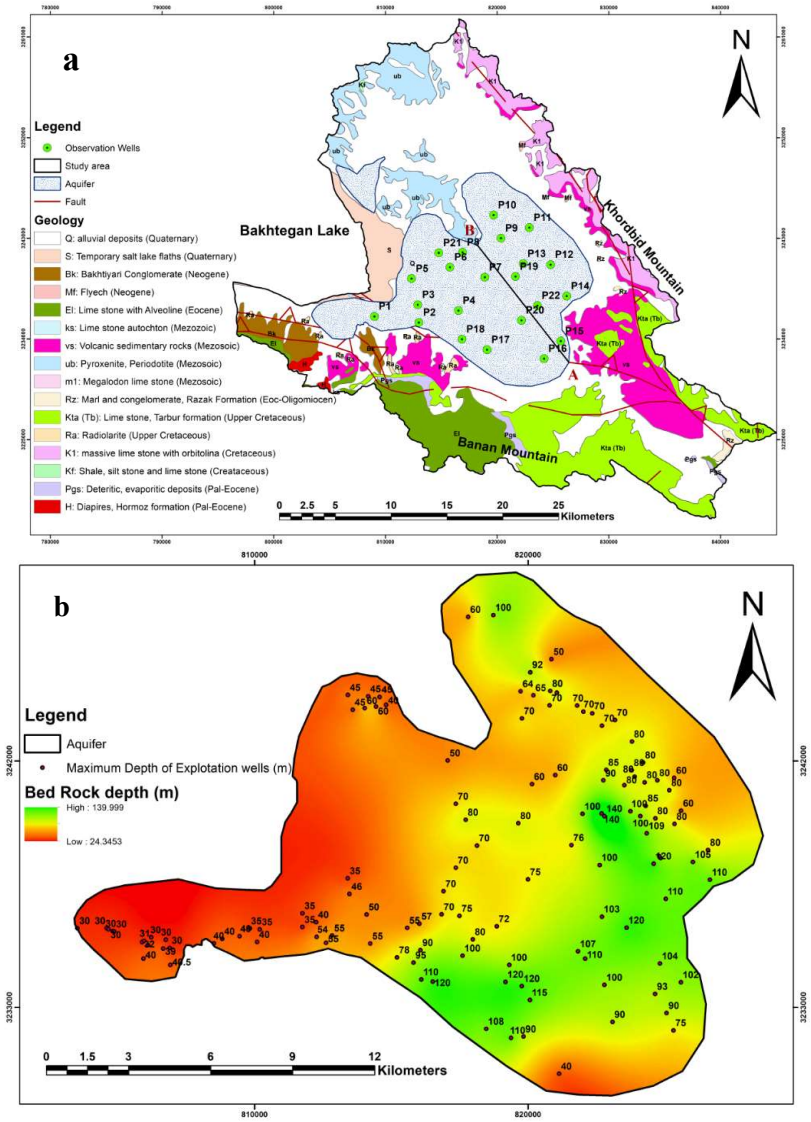

Figure 2. The geological map of the study area, along with the location of the aquifer and its observation wells (a), as well as the maximum probable bedrock depth map (in meters) of the aquifer (b) are shown, including the location and depth of selected EWs

Table 1. The OWs name, UTM, depth, water levels in Sep 1995 and 2020 and the statistical water level parameters

OW name	X	Y	Water Level (WL) in meter			statistical WL parameters (m)		
			Top Level of OW	WL in Sep 1995	WL in Sep 2020	Average	Maximum	minimum
P1	225701	3235126	1572.89	1558.69	1550.96	1554.50	1559.74	1550.74
P2	229644	3234382	1580.18	1548.23	1541.31	1544.07	1549.58	1540.28
P3	229630	3235976	1570.02	1551.62	1543.19	1546.93	1552.57	1542.75
P4	233240	3235267	1580.96	1545.66	1537.33	1540.46	1548.26	1532.98
P5	229188	3238335	1567.89	1559.50	1548.18	1553.61	1559.50	1548.18
P6	232680	3239177	1573.73	1556.33	1538.58	1544.36	1556.33	1538.06
P7	235752	3238127	1580.77	1539.06	1526.35	1529.17	1539.12	1517.07
P8	233879	3240449	1576.21	1559.79	1533.91	1543.79	1560.31	1531.71
P9	237368	3241531	1583.60	1538.95	1515.99	1524.67	1539.30	1514.93
P10	236820	3243627	1589.95	1542.25	1514.95	1528.30	1544.80	1514.95
P11	239954	3242347	1588.73	1541.82	1534.99	1534.65	1545.32	1529.32
P12	241685	3238949	1590.51	1530.26	1545.81	1522.45	1545.81	1508.32
P13	239228	3239152	1586.02	1533.72	1510.71	1520.28	1536.25	1509.58
P14	242980	3236064	1603.77	1535.85	1525.20	1526.40	1540.54	1516.04
P15	242246	3232072	1621.37	1579.03	1564.34	1562.99	1589.43	1550.42
P16	240670	3230585	1624.61	1603.62	1600.73	1596.70	1605.37	1592.44
P17	235615	3231641	1604.37	1555.75	1534.18	1533.53	1564.09	1520.40
P18	233423	3232699	1603.45	1526.97	1529.10	1524.09	1530.32	1520.80
P19	238496	3238046	1585.88	1532.38	**Dry**	1522.89	1532.38	1519.15
P20	238831	3234110	1599.16	1546.42	1516.26	1524.83	1549.76	1508.65
P21	231748	3240508	1570.57	1553.17	1544.59	1548.40	1553.32	1544.58
P22	240315	3235345	1597.28	1597.28	1508.85	1546.40	1597.28	1497.42

ArcGIS approach

The ArcGIS 10.6.1 software is used for drawing maps and calculating aquifer volume and thickness. The aquifer volume is calculated in ArcGIS using the spatial analysis toolbox and the Cutfill command. For this we need two rasters: the bedrock and the water level. The bedrock raster is obtained from the minimum well level (maximum well depth) in the regions shown in Fig. 2b. The water level raster is the interpolated water level in OWs from September 1995 to 2020. The aquifer thickness is calculated in ArcGIS using the spatial analysis toolbox and the Raster Calculator command. In this command, the bedrock level is subtracted from the water level of September 1995, 2001, 2006, 2011, 2016, and 2020 to determine the aquifer thickness for those respective years.

Results and discussion

Results of hydrogeology and hydrochemistry

In this section, the results of the hydrogeology and hydrochemistry of the study area were determined by the iso-potential and iso-EC lines map, hydrograph and chemograph, the cross section and Piper, Schoeller, Durov, and Gibbs diagrams. Figure 3 displays the iso-potential lines in Sep 1995 (a) and in Sep 2020 (b) with their corresponding flow lines (Table 1 data). The freshwater flow lines in the Neyriz plain are from southeast to northwest entirely. In Sep 1995, the flow lines in the west and north parts are from northwest to southeast (from Bakhtegan salt Lake to the aquifer) towards the middle of the aquifer. This may indicate saltwater intrusion from Bakhtegan Lake, which requires further geochemical study for confirmation. In Sep 2020, with a water level drawdown of about 10 meters in the aquifer, the flow lines in the south and

southeast of the aquifer are from southeast to northwest, and the flow lines in the northeast are from east to west. Along the western part of the aquifer, the Bakhtegan saltwater intrusion occurred. From these two figures, we can conclude that the Tarbur limestone in the southeast of the aquifer recharges the groundwater consistently. Therefore, the water level in this recharge zone remains unchanged despite the 10-meter drawdown of the aquifer. Additionally, the drawdown in the aquifer has led to another recharge from the northern massive Orbitolina limestone. The iso-EC lines in Sep 1998 and 2020 are shown in Fig. 4 (Table 2 data). As shown in Fig. 4a, a decreasing trend of EC is observed from Bakhtegan Lake towards the recharge zones. This figure confirms the flow entrance from the southeast side towards the aquifer (the lowest EC value is in the recharge zone of the aquifer in Fig. 3a), and the EC value increases along the flow line. Maximum EC values exist in the western part of the aquifer (closest part to Bakhtegan Lake). In Fig. 4b, in Sep 2020, the EC values increased in the central and western parts of the aquifer. The maximum EC values of about 12000 in Sep 1998 that existed in the western part of the aquifer were observed in the central part in Sep 2020, indicating further saltwater intrusion from Bakhtegan salt Lake. The cross section of the water table and its EC along line AB in Figure 2a are shown in Fig.5.

Table 2. The EWs name, UTM and EC in Sep 1998 and 2020 and the long term statistical EC parameters

Row	EW name	X	Y	EC (µS/cm)				
				Sep-98	Sep-20	long term parameters		
						Average	Maximum	Minimum
1	**W1**	221483	3235105	3783	10448	7442.36	26548	3283
2	**W2**	222520	3234653	16075	11561	21417.9	37310	5424
3	**W3**	223759	3234682	15342	10276	10376.4	20080	4337
4	**W4**	224882	3247701	7864	10276	9420.1	15355	3829
5	**W5**	225137	3234473	5208	6894	7000.14	12221	2732
6	**W6**	225238	3247428	3715	8135	12241.9	26566	3140
7	**W7**	225978	3246920	3622	10105	8715.45	26646	3581
8	**W8**	229576	3234979	1333	547	1098.27	1730	547
9	**W9**	229616	3236853	372	480	544.391	3313	308
10	**W10**	230830	3243070	2100	3483	2152.8	3725	1413
11	**W11**	230831	3234171	5024	9334	5831.7	10710	3680
12	**W12**	232281	3234358	1615	9420	6666.12	13293	1615
13	**W13**	232668	3233776	650	582	664.598	984	463
14	**W14**	234096	3240118	1615	2141	1734.42	2742	820
15	**W15**	234355	3232155	655	557	631.797	921	432
16	**WP1**	234591	3238538	4410	11989	8977.76	15200	3824
17	**WP2**	235533	3230985	6298	5780	7492.74	11304	3220
18	**WP3**	235692	3233558	-	11133	9934.56	14317	6680
19	**WP4**	235816	3237552	5249	11989	9897.36	16380	4054
20	**WP5**	236756	3230884	12516	17220	12964.9	29825	4860
21	**WP6**	236773	3245101	7500	11989	9469.94	18329	3511
22	**WP7**	237253	3236902	-	10448	12232.3	21801	8302
23	**WP8**	237295	3244260	7100	9848	10398.1	15367	6985
24	**WP9**	238135	3242964	6020	9420	10258.4	20553	4021
25	**WP10**	239354	3241856	5900	14274	10970.1	19635	5060
26	**WP11**	239700	3239321	7956	9564	11588	19929	6171
27	**WP12**	239812	3240057	3957	10705	7974.1	16635	3475
28	**WP13**	240422	3242208	1665	2389	2223.6	3703	1634
29	**WP14**	240661	3231588	-	6585	3620.82	7880	1805
30	**WP15**	241425	3236135	2907	4873	4191.56	7200	2191
31	**WP16**	241607	3239135	3715	15702	6139.48	15850	1474
32	**WP17**	242110	3232174	6373	11903	11781.9	22547	5956
33	**WP18**	242667	3228992	751	531	682.576	831	427

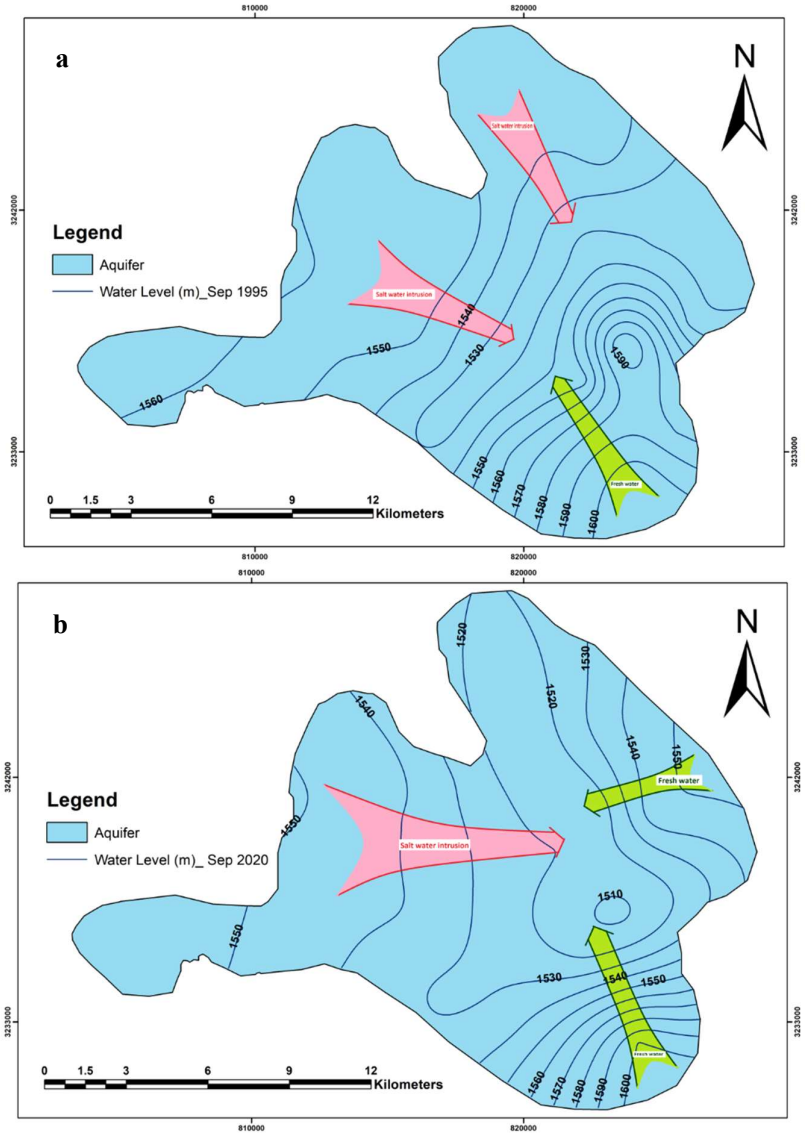

Figure 3. The iso-potential lines of water level (m) and flow lines in Sep 1995 (a) and in Sep 2020 (b). The red arrow shows the saltwater intrusion, while the green arrow shows the direction of fresh water flow based on the iso-potential lines

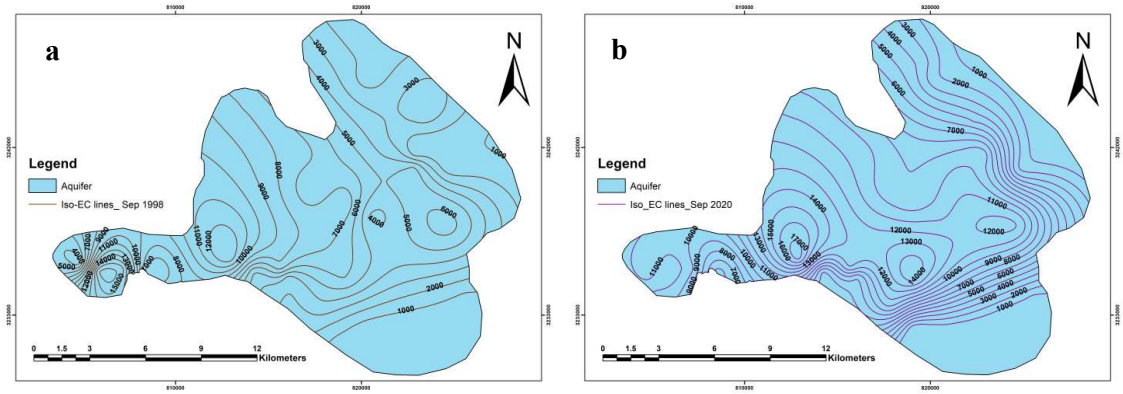

Figure 4. The iso-EC lines (µS/cm) in Sep 1998 (a) and in Sep 2020 (b)

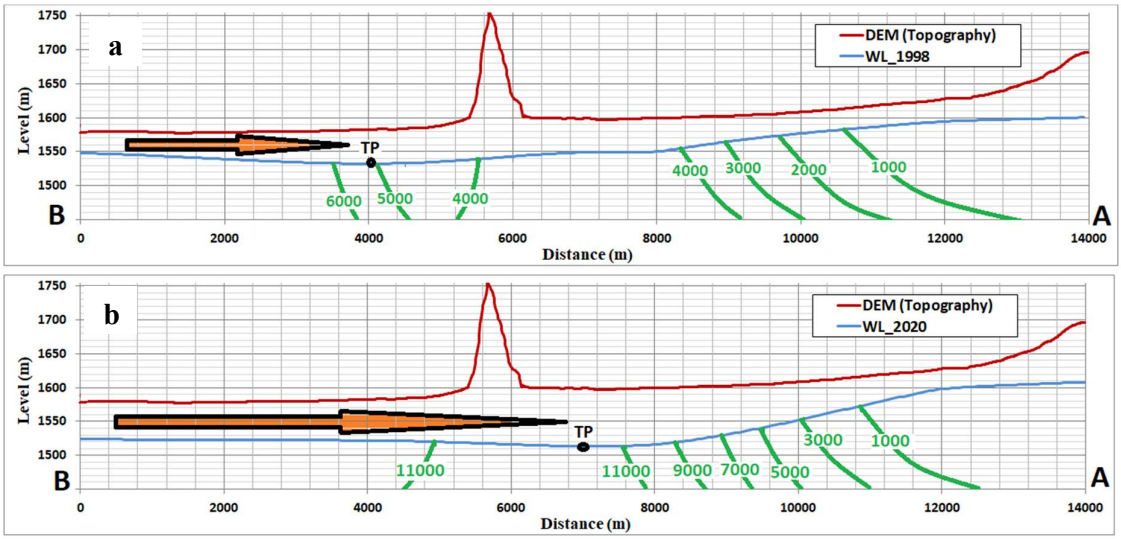

Figure 5. The cross section along line AB in Fig. 2a shows the topography line (brown line), water level line (blue line), TP (black circle), and EC contours (green line) in 1998 (a) and 2020 (b). Since data on the depth variation of electrical conductivity was not available, the depth curvature of the electrical conductivity contours is schematically plotted. The orange arrow indicates the intrusion of saltwater into the lake, based on the slope of the water level

According to the DEM file of the area, there is a hill with a height of about 150 meters along line AB. In this figure, the water table in 1998 and 2020 and the EC values based on Figures 3 and 4 are plotted. As the figure shows, the increasing extraction of groundwater resources (mismanagement of groundwater) and the reduced recharge of the aquifer due to climate change have led to a greater drawdown of the aquifer (especially in middle part that may cause from well field) and the gradient of the water table near the lake has reversed. In other words, the lowering of the water table in the aquifer has led to the direct intrusion of salt water from the lake into the aquifer. In each diagram, the turning point of the water table (TP) was calculated and plotted in order to determine the length of the surface saltwater intrusion front using equipotential lines. In 1998, the lake saltwater entered the aquifer along line AB of about 4000 meters, which increased to about 7000 meters in 2020 (175 percent increased). In order to plot the depth of the iso-EC lines, it was necessary to measure the EC change with respect to depth at several points in the area. Since this information is not available in the study area, the depth curvature of the iso-EC lines is drawn schematically. In both cross sections, the EC value in recharge zone (around A) is almost constant. The increase in EC of the groundwater from point A to TP is due to deep saltwater intrusion into the aquifer from below (Todd & Mays, 2005). In 2020, the increase in the EC of water from point A to TP shows a sharp increase (almost twice), possibly due to the decrease in groundwater recharge and the intensive extraction of groundwater by wells from 1998 to 2020, which leads to a strong intrusion of salt water from below into the aquifer. Figure 6 presents the hydrograph (a) and chemograph (b) of the Neyriz aquifer along with the Neyriz rain gauge station. The hydrograph shows a 10.08 meter drawdown from 1994 to 2020 (an annual drawdown of about 0.4 meters), with some compensation for the aquifer drawdown from 2016 to 2020.

In Fig. 6a, the water level from Sep 1995 to 2012 lowered about 13 meters, and from 2012 to Sep 2016, it remained stable with monthly changes. In Feb 2017, the greatest rainfall (177 mm) during the statistical period occurred, leading to a rising trend of the water level until Sep 2020. This indicates that artificial recharge in this plain would be beneficial to compensating the drawdown in the aquifer. In Fig. 6b, the hydrograph and chemograph are plotted on the same figure. Since the EC data are not monthly (mainly measured in dry and wet seasons or

once every three months), the chemograph is plotted as scattered points. Generally, when the water level decreases, the EC value rises, and vice versa. However, the total EC values in this aquifer show a rising trend even from 2012 to 2016 or 2017 to 2020, where the aquifer water level remained stable and showed a rising trend, respectively. It is evident that the EC data exhibit two trends, one from 1995 to Jan 2012 and the other from Apr 2012 to Sep 2020. Therefore, we can conclude that the increasing trend of EC values despite stable and rising trends of the water level from 2012 to 2020 may be due to saltwater intrusion from Bakhtegan salt Lake. Figure 7 illustrates the location of EWs (Fig. 7a) for total analysis (Table 3), Durov (Fig. 7b), Piper (Fig. 7c and d), and Schoeller (Fig. 7e and f) diagrams of the aquifer. In the Durov diagram of EWs samples (Fig. 7b), the W9, 10, 13, 14, and 15 samples are close to each other and exhibit the same pattern. By comparing these sample locations (in Fig. 7a) and flow lines (Fig. 3), it is evident that all of them are along the recharge zone and close to limestone formations. Piper diagrams are plotted for Nov 2004 (Fig. 7c) and Dec 2018 (Fig. 7d). In Fig. 7c, the W9, 13, and 15 samples are very close to each other, contributing to the major recharge of the aquifer from the southern part of Tarbur limestone. Subsequently, the W8, 10, and 14 are close to them, near the recharge area from limestone formations. In Fig. 7d, most samples in Dec 2018 have higher Cl and SO4 in anions and lower Ca and Mg in cations. The water type of each sample is listed in Table 3. As shown in this table, only the EWs samples along the recharge zone from limestone formations have bicarbonate water type.

Table 3. Results of the chemical analysis of the groundwater samples in Neyriz Plain

Sample	Date	Ca (epm)	Mg (epm)	Na (epm)	K (epm)	HCO3 (epm)	SO4 (epm)	Cl (epm)	EC (µS/cm)	pH	Water type
W1	Nov-04	37	46	74	0.28	2.45	12.5	152	13299	7.25	Mg-Cl
W2	Nov-04	9	13	34.8	0.15	3.75	22.75	31	6483	7.65	Na-Cl
W3	Nov-04	37	46	74	0.28	2.45	12.5	152	13299	7.25	Mg-Cl
W4	Nov-04	35	25	23	0.17	2	7.5	75	7501	7.3	Mg-Cl
W5	Nov-04	16	28	37	0.33	1.9	20	66	7273	7.5	Mg-Cl
W6	Nov-04	51	34	6.4	0.08	1.9	1	90	8229	7.43	Mg-Cl
W7	Nov-04	7.85	7.15	2.45	0.05	2	1.5	14.4	1766	7.93	Mg-Cl
W8	Nov-04	2.2	6.05	2.88	0.05	3.9	4.55	2.6	997	8.16	Mg-SO4
W9	Nov-04	1.6	1.7	0.83	0.02	2.9	1	0.6	366	8.15	Mg-HCO3
W10	Nov-04	2.65	2.45	7.57	0.03	2.8	6.25	3	1122	8.2	Na-SO4
W11	Nov-04	23	17	12	0.08	2	8.75	41	4696	7.62	Mg-Cl
W12	Nov-04	37	13	6.7	0.07	1.5	2	52	5403	7.52	Ca-Cl
W13	Nov-04	2	1.9	2.58	0.03	2.95	1.31	1.8	607	8.42	Mg-Cl
W14	Nov-04	2	2.3	9.74	0.06	3.2	10	1.2	1496	8.38	Na-SO4
W15	Nov-04	2.8	0.7	1.5	0.03	2.85	1	0.8	432	8.35	Ca-HCO3
W1	Dec-18	23.25	19.75	42.87	0.45	4	9.54	72.25	8478	7.57	Na-Cl
W2	Dec-18	35.5	38.5	73.5	1.1	4	7.9	135	14413	7.2	Na-Cl
W3	Dec-18	30	30.5	81.02	0.98	4	6.88	130	14203	7.51	Na-Cl
W4	Dec-18	30	35.25	54.97	0.95	1.65	7.96	112.5	12103	8.05	Mg-Cl
W5	Dec-18	48	32	18.31	0.5	2.5	6.16	89	9559	7.36	Mg-Cl
W6	Dec-18	50.5	39	22.14	0.5	2.5	15.27	92.5	10400	7.28	Mg-Cl
W7	Dec-18	46	47.5	33.69	0.97	2.8	7.35	120	12194	7.69	Mg-Cl
W8	Dec-18	3.8	2.1	4.7	0.05	4.5	3.72	2.5	1035	7.63	Na-SO4
W9	Dec-18	2.6	2.3	1.07	0.03	3.95	0.83	1.2	596	7.71	Mg-HCO3
W10	Dec-18	5.7	3.35	12.06	0.09	3.1	11.63	5.25	1918	7.65	Na-SO4
W11	Dec-18	43.25	22	13.36	0.35	2.1	7.32	70	7876	7.43	Ca-Cl
W12	Dec-18	44.5	24.75	14.98	0.46	2.2	9.77	73.25	8475	7.36	Ca-Cl
W13	Dec-18	3.9	1.25	1.56	0.04	4.15	0.97	1.6	658	7.64	Ca-HCO3
W14	Dec-18	5.5	6.3	9.81	0.11	3.1	9.76	8.1	2119	7.63	Mg-Cl
W15	Dec-18	3.65	1.4	0.91	0.03	4.35	0.72	0.9	591	7.58	Ca-HCO3

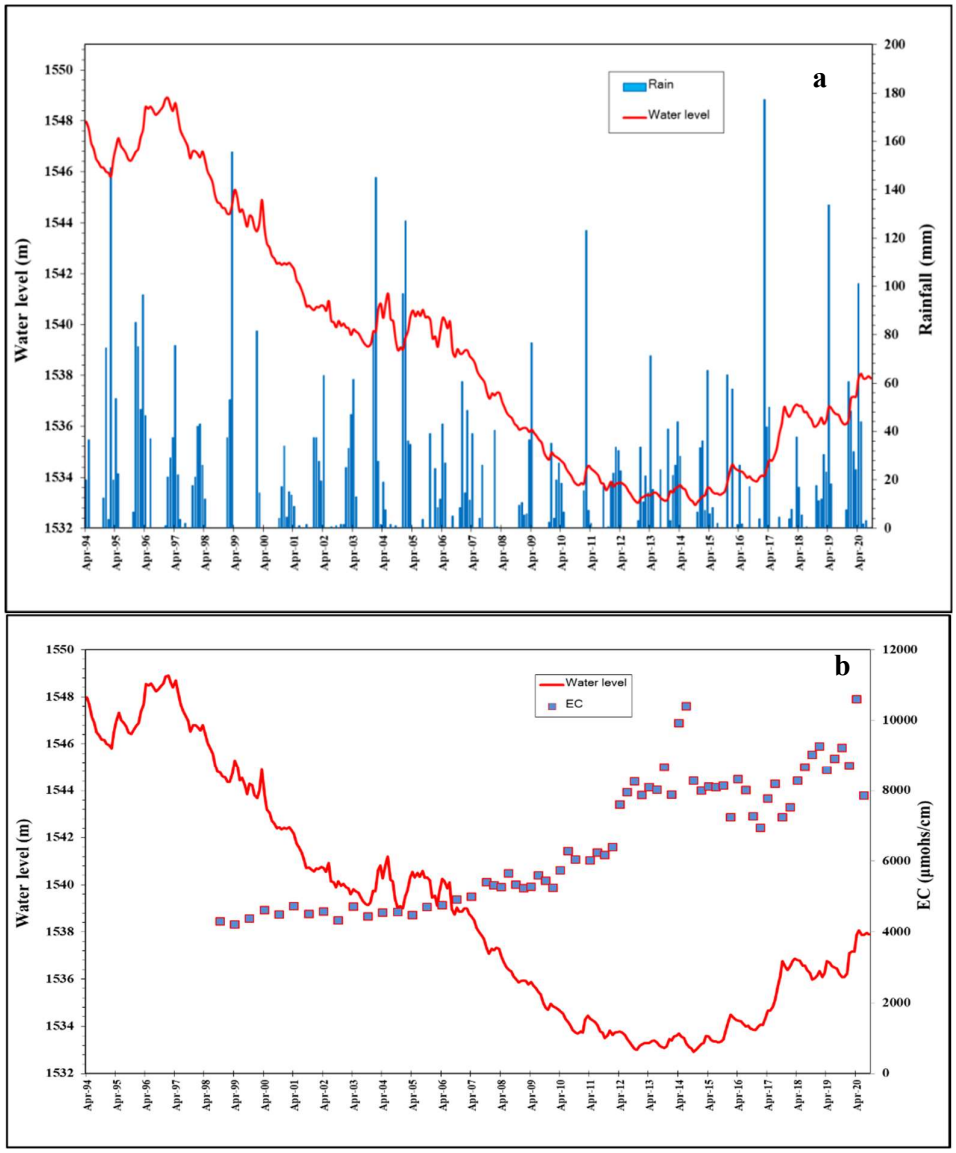

Figure 6. The hydrograph of Neyriz plain with the monthly Neyriz rain gauge station data (a) and chemograph of Neyriz plain with the hydrograph (b)

The Schoeller diagram is presented in Fig. 7e and f. In these figures, the W9, 13, and 15 lines are lower than other samples and slightly parallel to each other, indicating the same source of water (recharge from limestone formations). Other samples closest to them, W8, 10, and 14, exhibit the same trend and reveal the recharge zone. Other samples show similar trends, indicating the effect of saltwater intrusion. The Gibbs plot is shown in Fig. 8 in 2004 (a) and 2018 (b). In Fig. 8a, the W8, 9, 10, 13, 14, and 15 samples along the southeast and north of the aquifer are in the rock-dominant part of the aquifer. Among these samples, W10, 8, and 13 have more distance from others, suggesting they are close to the mixing zone of the aquifer. The other samples (W1, 2, 3, 4, 5, 6, 7, 11, and 12) are predominantly in the saltwater intrusion part of the aquifer. After 2018, W14 and W10 have taken the greatest distance from these samples, indicating the mixing zone of fresh and saltwater. In other words, W14 and W10 have been more affected by saltwater intrusion than the other samples, showing the entry of the saltwater front into their vicinity. The remaining samples (W1, 2, 3, 4, 5, 6, 7, 11, and 12) move towards the right corner of the plot and are very close to each other, indicating saltwater intrusion on all of them.

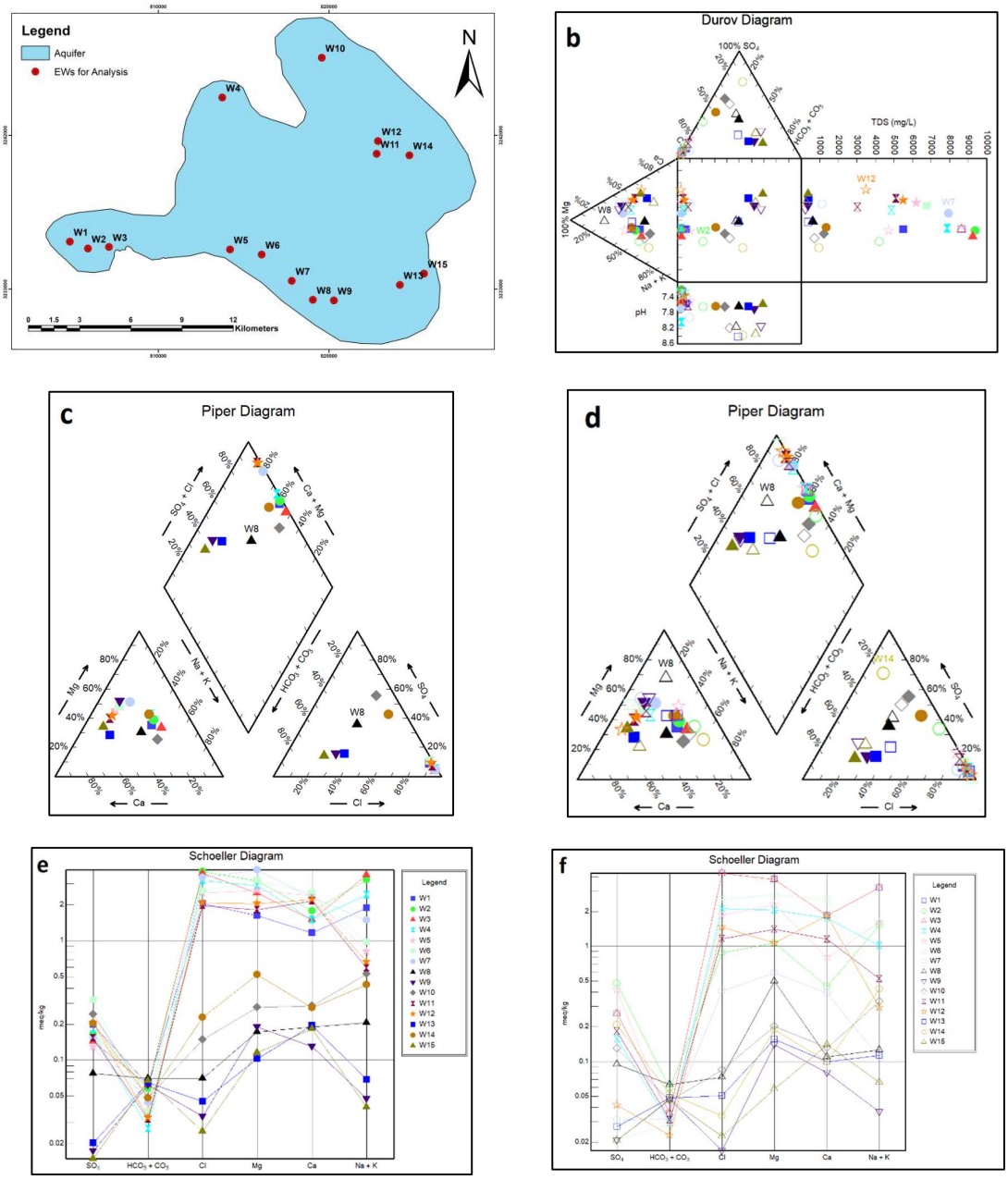

Figure 7. a) The locations of EWs for analysis (in Tables 2 and 3), b) the Dourv diagram for the years 2004 and 2018, c) the Piper diagram of the 2018 data, d) the Piper diagram of the 2018 and 2004 data, e) the Schoeller diagram of the 2018 data, and f) the Schoeller diagram of the 2004 data. It should be noted that solid shapes represent the W_1 to W_8 samples in 2018, while hollow shapes represent their equivalents in 2004. The figures legend is shown in figures e and f

Results of the groundwater volume

The groundwater volume in Neyriz plain was calculated from September 1995 to 2020 and is illustrated in Fig. 9. As can be seen in this figure, the aquifer volume follows the same trend as the water level until 1998. After that, with a significant decrease in the water level, the aquifer volume decreased as well. This decrease in the water level mainly occurred in parts of the aquifer with the smallest thickness. The aquifer volume was 7020.02 MCM in September 1995

and decreased to 4002.37 MCM in September 2020. Therefore, the aquifer volume decreased by 3017.65 MCM over 25 years, which averages to an annual decrease of 120.71 MCM in aquifer volume. Taking into account the aquifer area of 234.9 square kilometers, the annual drawdown of the water level would be 0.51 meters, which is very close to the 0.4 meters annual drawdown of the water level calculated from the hydrograph. The relationship between aquifer volume and water level is best represented by a linear fit, as shown in Fig. 10a. The relationship between aquifer volume and water level depends on many factors, such as aquifer geometry, changes in porosity with depth, and variations in aquifer materials. In this research, an empirical linear equation exists between aquifer volume and water level with over 95 percent precision. The linear equation is as follows:

$$V = 300.3H - 457205 \qquad H>1523 \qquad (1)$$

In this equation, V represents the aquifer volume (MCM) and H represents the hydrograph water level (m) that is more than 1523. Therefore, using this equation, users can calculate the aquifer volume based on the water level in Neyriz Plain. In Figure 10b, the EC values of the aquifer in relation to the aquifer water level are plotted, showing that as the aquifer water level decreases, EC values increase. Two trends can be identified in this figure: one for aquifer water levels greater than 1538 meters (shown with red points in Figure 10a and b) and another for aquifer water levels less than 1538 meters (shown with blue points in Figure 10a and b).

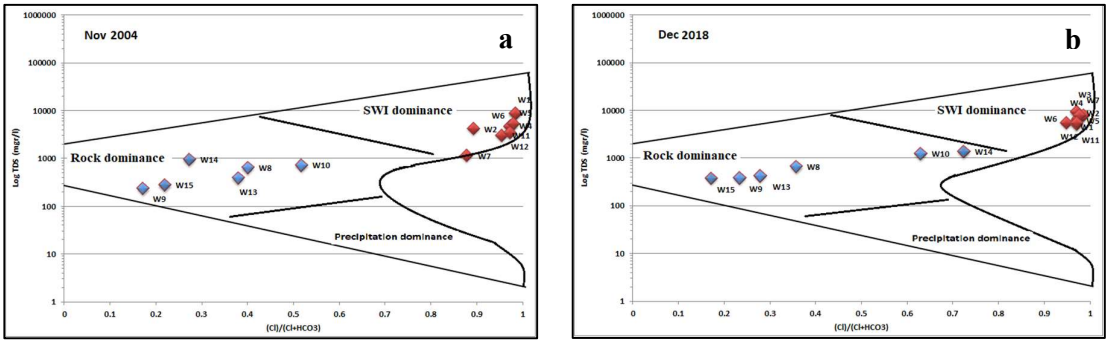

Figure 8. Gibbs plot of data in 2004 (a) and 2018 (b)

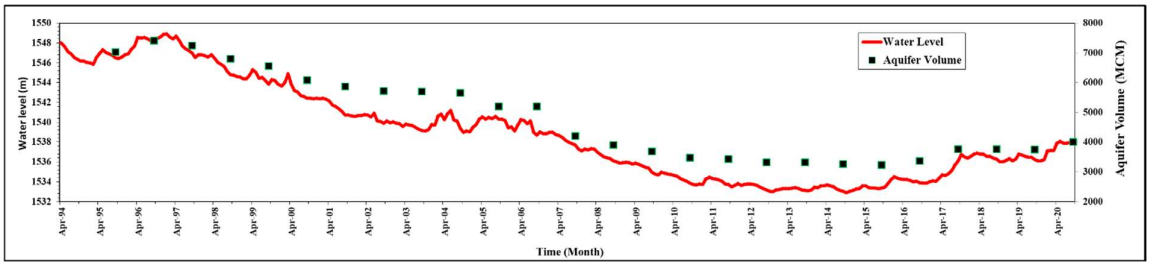

Figure 9. The water level and aquifer volume of Neyriz aquifer during 1994 to 2020

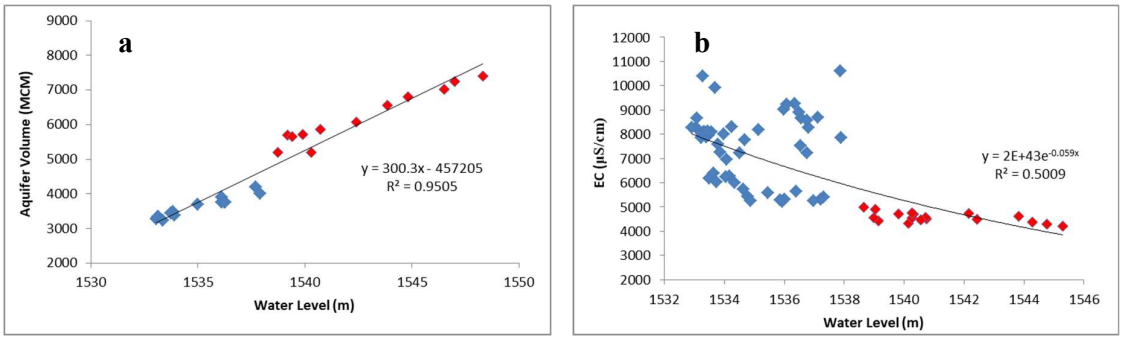

Figure 10. The aquifer volume (a) and EC changes (b) respect to the water level and their best fit

Along the first trend, EC values decrease linearly as the aquifer water level increases, while in the second trend, EC values are high and do not follow a specific trend. On the basis of these findings, let us take a closer look at Figures 9 and 10a. Figure 10a show that the volume of the aquifer decreases sharply when the water table drops below 1538 meters, and that the linear best fit shows an even less pronounced downward trend. This could be due to the decrease in volume of the aquifer in areas where the bedrock has a lower gradient. To further elaborate on this topic, Figure 11 shows the bedrock level (based on the information from Figure 2b and the DEM of the area) together with the bedrock level contour lines at 1536, 1538 and 1540 meters. It can be seen from this figure that when the water table in the aquifer drops from 1540 meters to 1538 meters, the northern, northeastern and southern parts of the aquifer experience only minimal changes in their lateral boundaries due to the steep gradient of the bedrock. The decrease in the volume of the aquifer in these areas is solely due to the lowering of the water table. However, in the western part of the aquifer (western nose of the aquifer), where the bedrock has a lower gradient, the lateral boundary of the aquifer contracts (causing part of the aquifer to dry out due to the lowered water table reaching the bedrock). This change becomes even more pronounced when the water table drops to 1536 meters. It can therefore be deduced from Figure 11 and the results of Figures 9 and 10 that a rise in the water table from 1538 meters to 1540 meters expands the lateral boundary of the aquifer in its western part, leading to a considerable increase in aquifer volume and the decrease of salt water intrusion. Conversely, a drop in the groundwater level from 1538 meters to 1536 meters causes the lateral boundary of the aquifer in the western part to contract, leading to a significant decrease in aquifer volume and an increase in saltwater intrusion from the lake.

Results of changes in aquifer thickness

The thickness of the aquifer was calculated in this study in order to better understand changes in groundwater volume over time. The aquifer thickness for September 1995, 2001, 2006, 2011, 2016, and 2020 was calculated and plotted in ArcGIS (see Fig. 12). As shown in the figure, the aquifer thickness in September 1995 ranged from 0 to 120 meters, with the lowest thickness in the north, south, and west of the aquifer, and the highest thickness in the eastern part.

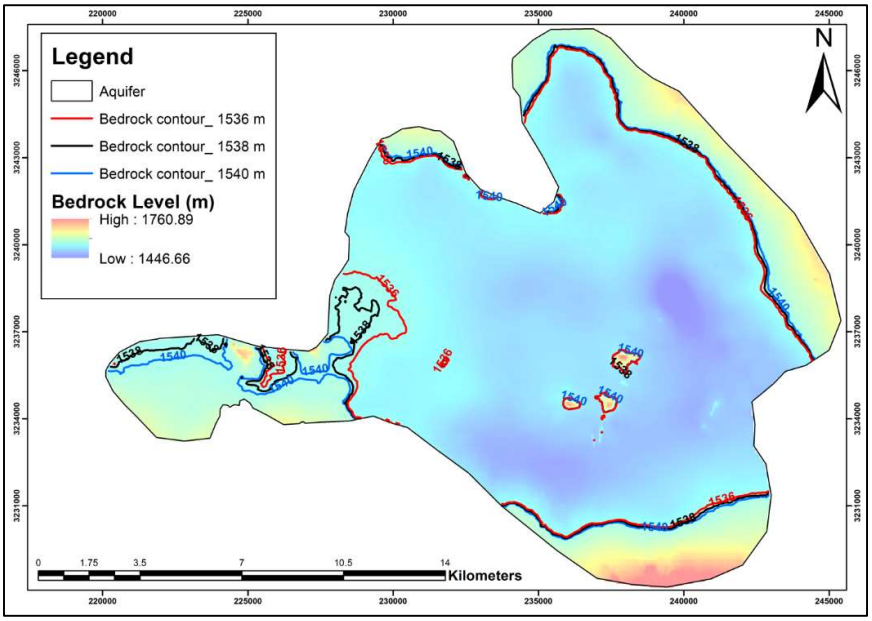

Figure 11. The bedrock level map of the aquifer with contour lines at 1536, 1538 and 1540 meters (with red, black and blue lines, respectively)

The aquifer thickness also indicates that the aquifer boundaries provided by the Regional Water Company of Fars are not entirely accurate and should be revised. From 1995 to 2016, the aquifer thickness decreased to 0 to 60 meters in most parts of the aquifer. However, from 2016 to 2020, the aquifer thickness in the southern part increased. These figures illustrate a decreasing trend in aquifer thickness from September 1996 to 2016 as could see this decreasing trend of water level in hydrograph (Fig. 6a). In September 2020, the northern, western, and southern parts of the aquifer, which have the lowest thickness, dried up, with aquifer thickness mainly less than 60 meters. In Fig. 12 (a), the Exploitation Wells (EWs) are shown along with aquifer thickness in September 2020. Most of the EWs are located in the southern and central parts of the aquifer, where there has been a greater decrease in aquifer thickness (less than 60 meters). Fig. 12 (b) displays iso-drawdown lines (in meters) of the aquifer from September 1995 to 2020. The highest drawdown values (more than 80 meters) occurred in the central and eastern parts of the aquifer.

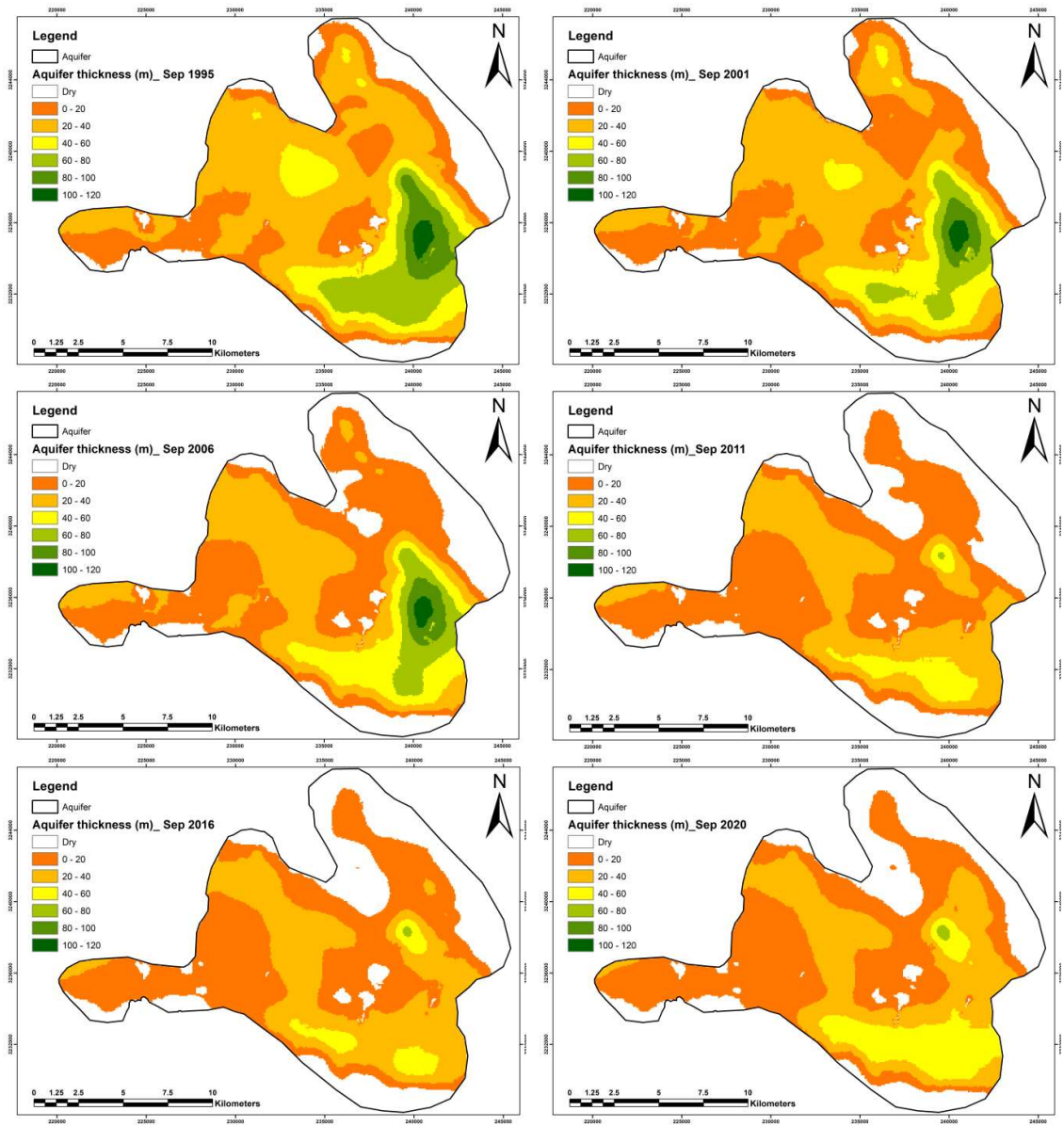

Figure 12. The thickness of the aquifer (in meters) changed in September of 1995, 2001, 2006, 2011, 2016, and 2020

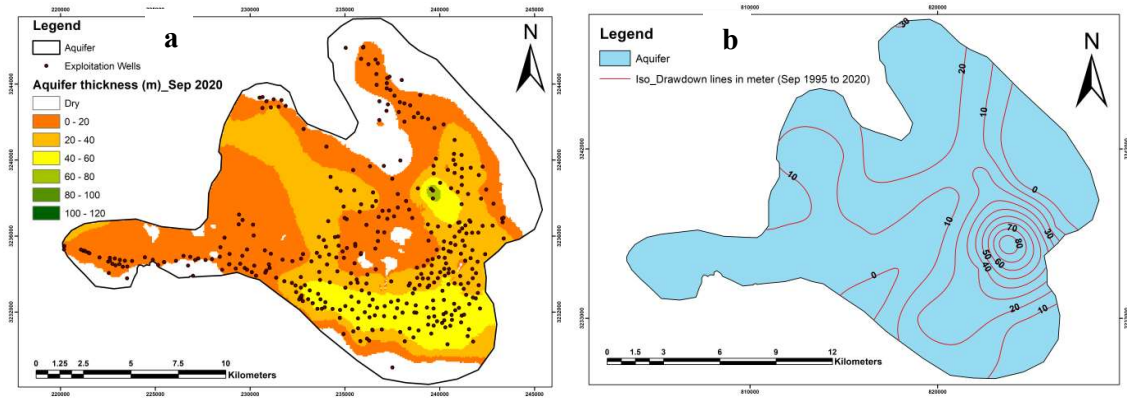

Figure 13. The thickness of the aquifer (in meters) in September 2020, as well as the exploitation wells (a) and iso-drawdown lines (in meters) of the aquifer from September 1995 to 2020 (b)

Conclusion

Poor management of groundwater resources and climate change have led to a water crisis in Iran. When making decisions about water resources in a region, it is crucial to understand the hydrogeological conditions of the area and the changes in the volume and thickness of the aquifers. The study area is located in the south of Iran in the Neyriz plain. The hydrograph of the aquifer shows a drawdown of 10.08 meters from 1994 to 2020 (an annual drawdown of about 0.4 meters), with some drawdown compensated from 2016 to 2020. Despite rising water levels from 2016 to 2020, the chemograph of the aquifer shows a deterioration in water quality. The highest precipitation during the statistical period fell in February 2017 (approx. 177 mm), which positively affected the rise in the aquifer's water level. Isopotential maps show that the flow lines run from southeast to northwest and west of the aquifer. In addition, saltwater intrusion from Bakhtegan Lake was observed from the west and northwest into the eastern part of the aquifer. The iso-EC lines show an increasing trend of EC along the flow lines, with the lowest EC values in the recharge zone of the aquifer (in the southeast and northeast of the aquifer). The cross-sectional plot of the changes in water table and EC along the AB line in 1998 and 2020 shows a lower water table in 2020 and a reverse gradient of the water table near the lake in both years. This is due to the increasing extraction of groundwater resources and the reduced recharge of the aquifer as a result of climate change. In addition, based on the TP of the water table in two cross sections, saltwater intrusion along the AB line is 4000 meters in 1998 and 7000 meters in 2020, representing a 175 percent increase. Additionally, the aquifer becomes salty after the A to TP due to saltwater intrusion from below. In this study, the volume of the aquifer was calculated and plotted for different years. It is clear from the various diagrams and analyses that the volume, water quality, and thickness of the aquifer change. The thickness of the aquifer also fluctuated over time, with the highest drawdown values occurring in the central and eastern parts of the aquifer. A linear empirical relationship was established between the volume of the aquifer and the water table. A graph was also produced showing the changes in electrical conductivity and aquifer volume as a function of water level. It was found that the aquifer behaves differently at levels above and below 1538 meters. In the analysis of the water table, it was found that significant changes in the lateral extent of the aquifer only occur in the western part (western nose) of the aquifer at levels above and below 1538 meters. This indicates a strong change in the volume of the aquifer, leading to a rapid entry of the saltwater intrusion into the aquifer and a shift in the trend of the EC in relation to the water level of the aquifer. From these results, it was concluded that the critical height of the aquifer level is 1538 meters. Given the positive response of the aquifer to the rainfall in February 2017, it is recommended to artificially recharge the aquifer and construct underground dams in the western part (western

nose) of the aquifer. Overall, more extensive geophysical studies are needed in the region to better understand the dynamics of the aquifer and make informed decisions about water resource management.

Conflicts of interest

Authors' contributions

Somayeh Zarei Doudeji conceived of the presented idea and developed the theory and performed the computations. Also, she supervised the findings of this work and discussed the results and writes the final manuscript.

References

Ahmadi, Z.S., Safavi, H.R., Zekri, M., 2020. Forecasting Groundwater Level under Climate Change and Water Resources Management Scenario. Journal of Water and Wastewater, 31(6): 34-47.

Aghanabati, A., 2004. Geology of Iran. Geology and Mineral Exploration Organization, 1: 1-856.

Al-Sheikh, O.N., and Al-Shamma'a, A.M., 2019. Using Geographic Information System (GIS) to estimate the volume of water for Al Dammam unconfined Aquifer within Al Salman basin, Al-Muthana Governorate, South West Iraq. Iraqi Journal of Science, 60(7):478-1485.

Ashofteh, P.S., Kalhori, M., Singh, V.P., 2024. Water resources management considering groundwater instability affected by climate change scenarios. Physics and Chemistry of the Earth, Parts A/B/C, 135: 1-15.

Ciampittiello, M., Marchetto, A., Boggero, A., 2024. Water Resources Management under Climate Change: A Review. Sustainability, 16: 1-14.

Earman, S., Dettinger, M., 2011. Potential impacts of climate change on groundwater resources – a global review. Journal of Water and Climate Change, 2(4):213-229.

Engelenburg, J.V., Hueting, R., Rijpkema, S., Teuling, A. J., Uijlenhoet, R., Ludwig, F., 2018. Impact of changes in groundwater extractions and climate change on groundwater-dependent ecosystems in a complex hydrogeological setting. Water Resources Management, 32: 259–272.

Ertürk, A., Ekdal, A., Gürel, M., Karakaya, N., Guzel, C., Gönenç, E., 2014. Evaluating the impact of climate change on groundwater resources in a small Mediterranean watershed. Science of The Total Environment, 499(15): 437-447.

Felisa, G., Panini, G., Pedrazzoli, P., Di Federico, V., 2022. Combined Management of Groundwater Resources and Water Supply Systems at Basin Scale Under Climate Change. Water Resources Management, 36: 915-930.

Franssen, H.J.H., 2009. The impact of climate change on groundwater resources. International Journal of Climate Change Strategies and Management, 1(3): 241-254.

Ghalamkari, S., Asadi, A., Pourkermani, M., 2019. Evaluation and exploration of groundwater resources by identifying the layer structure of the earth using the Electricity Earth method in the Roniz Plain; West Estahban. Journal of Water Resources Engineering, 12(40): 39-50.

Gorelick, S.M. and Zheng, c., 2015. Global change and the groundwater management challenge: Groundwater Management Challenge. Water Resources Research, 51(5):1-21.

Guermazi, E., Milano, M., Reynard, E., Zairi, M., 2019. Impact of climate change and anthropogenic pressure on the groundwater resources in arid environment. Mitigation and Adaptation Strategies for Global Change, 24: 73-92.

Hassan, W.H., Hossein, H.H., Nile, B.K., 2022. The effect of climate change on groundwater recharge in unconfined aquifers in the western desert of Iraq. Groundwater for Sustainable Development, 16(9): 21-36.

Hedayat, S., Zarei, H., Radmanesh, F., Mohammadi, A., 2021. Study of groundwater resources condition in plains of Bakhtegan-Maharloo basin. Nature and Science, 19(3):23-27.

Hosseini, M., Jahanshahi, R., Asadi, N., Nasiri, M., 2020. Qualitative investigation of groundwater resources in HassanAbad-Dehchah area, northeast of Neyriz, Fars province. Hydrogeology, 5(1): 150-165.

Jolly I., McEwan K.L., Holland K.L., 2008. A review of groundwater–surface water interactions in arid/semi-arid wetlands and the consequences of salinity for wetland ecology. Ecohydrology, 1(1):43-58.

Kumar, C.P., 2012. Climate change and its impact on groundwater resources. International Journal of Engineering and Science, 1(5): 43-60.

Li F., Feng P., ZhangW., Zhang T., 2013. An integrated groundwater management mode based on control indexes of groundwater quantity and level. Water Resources Management, 27(9):3273-3292.

Lo´aiciga, H.A., 2009. Long-term climatic change and sustainable ground water resources management. Environmental Research Letter, 4: 1-11.

Moradi, H., Nikzad, M., 2024. Human Interaction with Arid and Semi-Arid Environments: A Reflection on Traditional Methods of Water Management and Exploitation in Neyriz Plain, Fars Province, Iran. Parseh Journal of Archaeological Studies, 7(26): 339-362.

Ostad-Ali-Askari, K., Ghorbanizadeh Kharazi, H., Shayannejad, M., Zareian, M. J., 2019. Effect of management strategies on reducing negative impacts of climate change on water resources of the Isfahan–Borkhar aquifer using MODFLOW. River Research Application, 35: 611-631.

Saemi, E., Kamali, G.H., 2009. Balance calculation methods and optimal management of Neyriz plain water resources. The second national conference on the effects of drought and ways to manage it. 20 May. Esfahan.

Shamir, E., Megdal, S.B., Carrillo, C., Castro, C.L., et al., 2014. Climate change and water resources management in the Upper Santa Cruz River, Arizona. Journal of Hydrology, 521: 18-33.

Şimşek, C., Demirkesen, A.C., Baba, A., Kumanlıoğlu, A., Durukan, S., Aksoy, N., Demirkıran, Z., Hasözbek, A., Murathan, A., Tayfur, G., 2020. Estimation groundwater total recharge and discharge using GIS-integrated water level fluctuation method: a case study from the Alaşehir alluvial aquifer Western Anatolia, Turkey. Arabian Journal of Geosciences, 13:143.

Sorkhabi, O., Kurdpour, I., Sarteshnizi, R., 2022. Land subsidence and groundwater storage investigation with multi sensor and extended Kalman filter. Groundwater for Sustainable Development, 19:1-7.

Todd, D.K., Mays, L.W., 2005. Groundwater hydrology. Wiley, 3: 1-636.

Vahidipour, M., Raeisi, E., Zee, S., 2021. Active salt water intrusion of shrinking Bakhtegan-Tashk Lakes in South Iran threatens the freshwater resources of coastal aquifers. Journal of Hydrology:Regional studies, 34: 1-19.

Wahyuni, S., Oishi, S., Sunada, K., 2008. The estimation of the groundwater storage and its distribution in Uzbakistan. Annual Journal of Hydraulic Engineering, 52: 31-36.